

# Characterization and Methanol Electrooxidation Studies of Pt(111)/Os Surfaces Prepared by Spontaneous Deposition

Christina M. Johnston,<sup>†</sup> Svetlana Strbac,<sup>‡</sup> Adam Lewera,<sup>†</sup> Eric Sibert,<sup>§</sup> and Andrzej Wieckowski<sup>\*,†</sup>

Department of Chemistry, University of Illinois at Urbana-Champaign, Urbana, Illinois 61801, ICTM-Institute of Electrochemistry, University of Belgrade, 11001 Belgrade, Serbia and Montenegro, and Laboratory of Electrocatalysis, UMR CNRS 6503, University of Poitiers, Poitiers 86022, France

Received January 17, 2006. In Final Form: June 12, 2006

Catalytic activity of the Pt(111)/Os surface toward methanol electrooxidation was optimized by exploring a wide range of Os coverage. Various methods of surface analyses were used, including electroanalytical, STM, and XPS methods. The Pt(111) surface was decorated with nanosized Os islands by spontaneous deposition, and the Os coverage was controlled by changing the exposure time to the Os-containing electrolyte. The structure of Os deposits on Pt(111) was characterized and quantified by in situ STM and stripping voltammetry. We found that the optimal Os surface coverage of Pt(111) for methanol electrooxidation was  $0.7 \pm 0.1$  ML, close to  $1.0 \pm 0.1$  Os packing density. Apparently, the high osmium coverage Pt(111)/Os surface provides more of the necessary oxygen-containing species (e.g., Os–OH) for effective methanol electrooxidation than the Pt(111)/Os surfaces with lower Os coverage (vs e.g., Ru–OH). Supporting evidence for this conjecture comes from the CO electrooxidation data, which show that the onset potential for CO stripping is lowered from 0.53 to 0.45 V when the Os coverage is increased from 0.2 to 0.7 ML. However, the activity of Pt(111)/Os for methanol electrooxidation decreases when the Os coverage is higher than  $0.7 \pm 0.1$  ML, indicating that Pt sites uncovered by Os are necessary for sustaining significant methanol oxidation rates. Furthermore, osmium is inactive for methanol electrooxidation when the platinum substrate is absent: Os deposits on Au(111), a bulk Os ingot, and thick films of electrodeposited Os on Pt(111), all compare poorly to Pt(111)/Os. We conclude that a bifunctional mechanism applies to the methanol electrooxidation similarly to Pt(111)/Ru, although with fewer available Pt sites. Finally, the potential window for methanol electrooxidation on Pt(111)/Os was observed to shift positively versus Pt(111)/Ru. Because of the difference in the Os and Ru oxophilicity under electrochemical conditions, the Os deposit provides fewer oxygen-containing species, at least below 0.5 V vs RHE. Both higher coverage of Os than Ru and the higher potentials are required to provide a sufficient number of active oxygen-containing species for the effective removal of the site-blocking CO from the catalyst surface when the methanol electrooxidation process occurs.

## 1. Introduction

Fuel cells are portable, low-temperature, and nonpolluting power sources. The direct methanol fuel cell (DMFC) is a particularly attractive and heavily researched fuel cell candidate, but its performance is not yet acceptable due partly to inefficiencies of the present Pt-based anode and cathode catalysts. At the anode, the major pathway of methanol oxidation generates a CO intermediate, which poisons the Pt catalytic sites:



A well-known strategy for improving the properties of platinum is to add another metal (M) such as ruthenium, osmium, or iridium to increase the ability of the surface to remove the poisoning CO through the bifunctional mechanism:<sup>1,2</sup>



In addition to providing more oxygen-containing species, the admetal may induce electronic effects that weaken the CO bond

to platinum (the ligand effect).<sup>1,3–5</sup> Pt/Ru is currently the most active bimetallic catalyst, and it was developed commercially.<sup>1</sup> Recent efforts to improve anode catalysts have used ternary combinations of metals, and such ternary catalysts are more active than the Pt/Ru catalysts alone.<sup>6–8</sup> Beyond platinum and ruthenium, osmium is the third major component of these catalysts, but the interactions of Pt and Os have been studied much less than Pt and Ru.<sup>9</sup> Additionally, the popular and potent Pt/Ru catalyst needs a reactive reference point to shed more light, by comparison, on the Pt/Ru catalytic properties. Clearly, the Pt/Os system of a controlled geometry is the most suitable reference state to consider. Therefore, this study seeks to increase fundamental knowledge of the structure of Pt(111)/Os surfaces, and probes their ability to effectively activate methanol oxidation in view

(3) Chrzanowski, W.; Wieckowski, A. In *Interfacial Electrochemistry: Theory, Experiment, and Applications*; Wieckowski, A., Ed.; Marcel Dekker: New York, 1999; p 937.

(4) Lu, C.; Rice, C.; Masel, R. I.; Babu, P. K.; Waszczuk, P.; Kim, H. S.; Oldfield, E.; Wieckowski, A. *J. Phys. Chem. B* **2002**, *106* (37), 9581–9589.

(5) Ross, P. N., Jr. In *Electrocatalysis, Frontiers of Electrochemistry*; Lipkowsky, J., Jr., Ross, P. N., Eds.; Wiley-VCH Publishers: New York, 1998; Vol. 4, pp 43–74.

(6) Ley, K. L.; Liu, R.; Pu, C.; Fan, Q.; Leyarovska, N.; Segre, C.; Smotkin, E. S. *J. Electrochem. Soc.* **1997**, *144* (5), 1543–1548.

(7) Liu, R.; Iddir, H.; Fan, Q. B.; Hou, G. Y.; Bo, A. L.; Ley, K. L.; Smotkin, E. S.; Sung, Y. E.; Kim, H.; Thomas, S.; Wieckowski, A. *J. Phys. Chem. B* **2000**, *104* (15), 3518–3531.

(8) Reddington, E.; Sapienza, A.; Gurau, B.; Viswanathan, R.; Sarangapani, S.; Smotkin, E. S.; Mallouk, T. E. *Science* **1998**, *280* (5370), 1735–1737.

(9) Spendlow, J. S.; Wieckowski, A. *Phys. Chem. Chem. Phys.* **2004**, *6* (22), 5094–5118.

\* Corresponding author. E-mail: andrzej@scs.uiuc.edu.

<sup>†</sup> University of Illinois at Urbana-Champaign.

<sup>‡</sup> University of Belgrade.

<sup>§</sup> University of Poitiers.

(1) Hamnett, A., In *Interfacial Electrochemistry: Experimental, Theory and Applications*; Wieckowski, A., Ed.; Marcel Dekker: New York, 1999; pp 843–883.

(2) Watanabe, M.; Motoo, S. *J. Electroanal. Chem. Interfacial Electrochem.* **1975**, *60* (3), 275–83.

of the enhancement (bifunctional) mechanisms described above.<sup>10–13</sup> This study also provides a broad range of comparisons with Pt(111)/Ru.

A wider range of Os coverage is explored here than in our previous work that was carried out by electrochemistry and by predominately ex situ STM (in air). In this report, using an in situ STM, electrochemical, and XPS methods,<sup>10,11</sup> we report an observation that a high coverage of Os,  $0.7 \pm 0.1$  ML, is required for effective catalysis of methanol electrooxidation. This is indeed a high value and our discussions center around the meaning of this high value in methanol oxidation mechanisms. In parallel, we will demonstrate that expression of the Os uptake in terms of both coverage and packing density is needed for mechanistic understanding of the oxidation process on Pt(111)/Os. (The packing density is the ratio of the number of deposited Os atoms to the number of Pt(111) surface atoms.) XPS data were collected to account for the effect of the Os coverage on the Os oxidation state.

As mentioned above, taking the activity measurements together with the STM data, our present results are evaluated in the context of previous work on the Pt(111)/Ru substrates.<sup>1,14–17</sup> As for Pt(111)/Ru, we confirm that Pt(111)/Os substrates follow the bifunctional mechanism, but with significant differences in terms of the Os coverage and the optimal potential window for methanol electrooxidation. These differences most likely arise from the different oxophilicity of the Ru and Os metals under the specified electrochemical conditions, as concluded throughout the text and discussion below.

## 2. Experimental Section

Except where specifically noted, all measurements were carried out in 0.1 M H<sub>2</sub>SO<sub>4</sub>, and the potentials are reported versus RHE. Solutions were prepared using OsCl<sub>3</sub>·xH<sub>2</sub>O salt (Alfa Aesar), double-distilled H<sub>2</sub>SO<sub>4</sub> (GFS chemicals), and Milli-Q water. Methanol used was Fischer Optima grade. Electrochemical measurements were performed using an EcoChemie Autolab PGSTAT100. Spontaneous deposition of osmium on Pt(111) and Au(111) electrodes<sup>11,13,18,19</sup> was performed by exposing the electrodes to the aerated, aged (over two weeks) 0.1–1 mM OsCl<sub>3</sub> + 0.1 M H<sub>2</sub>SO<sub>4</sub> solution at open circuit potential (OCP) for the deposition times from 5 s to 6 h.

A Pt(111) single crystal 10 mm in diameter (MaTeck, Germany), cut and oriented to the accuracy better than 0.1° was used for in situ STM experiments. A Pt(111) single crystal and a Au(111) single crystal, both 6 mm in diameter (Accumet Materials, Ossining, New York), oriented to the accuracy better than 0.5°, were used for the voltammetry and chronoamperometry experiments. The Pt(111) crystals were annealed in the hydrogen flame for several minutes and cooled in a mixture of H<sub>2</sub> and Ar gases. The crystal, protected by a drop of ultrapure water, was transferred to an external electrochemical cell for the voltammetric and chronoamperometric measurements. For the in situ STM work, the Pt(111) surface was

additionally processed by the I<sup>−</sup>/CO treatment<sup>12,20</sup> as described in detail previously.<sup>13</sup> The Au(111) surface was prepared by heating the Au single crystal in butane flame and cooling in Ar atmosphere.

An 8 mm-Os ingot of 99.998% purity obtained from Equilon, Inc. (Midland, TX) was also used. The ingot was prepared by the supplier by smelting Os powder under Ar in a hydrogen furnace, and was polished in our laboratory with 80, 300, 600, 1200, and 2400 grit SiC paper sequentially, followed by fine grinding with 3 and 1 μm polycrystalline diamond suspension (Buehler). Despite the polishing procedure, the roughness factor was ≈10 times the geometric area calculated using the hydrogen adsorption/desorption charge. The real area was rather large due to the hardness and brittleness of Os, making it difficult to polish to mirror smoothness with the usual techniques. Additionally, the susceptibility of osmium to oxidation likely diminishes the reflectivity,<sup>21</sup> but the reflectivity did not significantly improve with attempts to reduce the surface to the metallic form electrochemically, indicating that the surface roughness was the primary cause of the dull appearance.

For collecting XPS spectra, an XPS (electrochemistry transfer) instrument equipped with an ESCA M-Probe high-resolution, multichannel hemispherical electron analyzer (Surface Science Instruments) was used.<sup>22</sup> A monochromatic Al Kα line ( $h\nu = 1486.6$  eV) operated at 110 W was used as the excitation source. The photoelectron energy was measured using the fixed analyzer transmission (constant pass energy) mode, with a constant pass energy of 25 eV, and the size of the incident X-ray beam was 800 μm. An S-Probe version of the 1.36 ESCA software (Fison Instruments) was used, and spectral peaks were fitted using a mixed Gaussian–Lorentzian line shape and Shirley baselines.

Scanning tunneling microscopy measurements were performed in situ using a Molecular Imaging (MI) PicoSPM. STM images were obtained using Apiezon wax-coated Pt–Ir tips in a constant current mode with the tunneling current between 1 and 3 nA. The tip bias was maintained between 0.2 and 0.4 V. The surface imaging potential was maintained in the region where Os was metallic,<sup>12</sup> that is, below 500 mV. The coverage of Os was determined as the fraction of the substrate area covered by Os islands in the respective STM images. Data analysis was achieved using the Visual SPM software from Molecular Imaging. Many of the Os islands were grouped closely together in the images. To determine the distribution of island heights, closely spaced islands were separated using the local minima present between them. Local minima were used because the STM tip does not return to the absolute minimum (the Pt surface) if the islands are too close together (ca. 0.5 nm for these data). The local minima were determined using line profiles. Such a precise island definition was not applied in our previous Pt(111)/Os STM work, which relied primarily on the absolute minimum.<sup>13</sup> Tip broadening effects were considered when calculating the island areas and island heights, based on the image sharpness at the steps. The Pt step height of ca. 0.24 nm<sup>23</sup> was used for direct comparison to the Os layers.

Working with surfaces of high Os coverage causes some practical issues with respect to reporting the Os coverage values. Surfaces with up to 9 layers of Os were prepared in this study, and STM images of such highly covered Pt(111) surfaces cannot clearly confirm or deny the exposure of the Pt substrate (and sites) to the solution phase. In such cases, the coverage cannot be reported in terms of ML. This necessitates the use of two descriptions of the Os coverage in this report: ML (from STM data) and packing density (from stripping voltammetry).

## 3. Results and Discussion

### 3.1. Pt(111)/Os Cyclic Voltammetry and XPS Results. After exposing a Pt(111) electrode to the Os-containing solution (0.1

(10) Crown, A.; Kim, H.; Lu, G. Q.; de Moraes, I. R.; Rice, C.; Wieckowski, A. *J. New Mater. Electrochem. Syst.* **2000**, 3 (4), 275–284.

(11) Crown, A.; Moraes, I. R.; Wieckowski, A. *J. Electroanal. Chem.* **2001**, 500 (1–2), 333–343.

(12) Rhee, C. K.; Wakisaka, M.; Tolmachev, Y.; Johnston, C.; Haasch, R.; Attenkofer, K.; Lu, G.-Q.; You, H.; Wieckowski, A. *J. Electroanal. Chem.* **2003**, 554–555, 367–378.

(13) Strbac, S.; Johnston, C. M.; Lu, G.-Q.; Crown, A.; Wieckowski, A. *Surf. Sci.* **2004**, 573, 80.

(14) Chrzanowski, W.; Wieckowski, A. *Langmuir* **1997**, 13 (22), 5974–5978.

(15) Gasteiger, H. A.; Markovic, N.; Ross, P. N., Jr.; Cairns, E. J. *J. Phys. Chem.* **1993**, 97 (46), 12020–12029.

(16) Iwasita, T.; Hoster, H.; John-Anacker, A.; Lin, W. F.; Vielstich, W. *Langmuir* **2000**, 16 (2), 522–529.

(17) Chrzanowski, W.; Wieckowski, A. *Langmuir* **1998**, 14 (8), 1967–1970.

(18) Chrzanowski, W.; Kim, H.; Wieckowski, A. *Catal. Lett.* **1998**, 50 (1, 2), 69–75.

(19) Strbac, S.; Behm, R. J.; Crown, A.; Wieckowski, A. *Surf. Sci.* **2002**, 517 (1–3), 207–218.

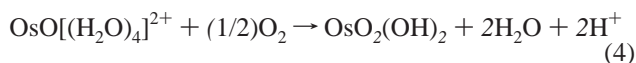
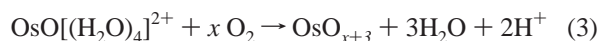
(20) Zurawski, D.; Rice, L.; Hourani, M.; Wieckowski, A. *J. Electroanal. Chem.* **1987**, 230 (1–2), 221–231.

(21) Pourbaix, M. *Atlas of Electrochemical Equilibria in Aqueous Solutions*; Pergamon Press: New York, 1966; p 638.

(22) Kim, H.; Rabelo de Moraes, I.; Tremiliosi-Filho, G.; Haasch, R.; Wieckowski, A. *Surf. Sci.* **2001**, 474 (1–3), L203–L212.

(23) Itaya, K. *Prog. Surf. Sci.* **1998**, 58 (3), 121–247.

or 1 mM  $\text{OsCl}_3 + 0.1 \text{ M H}_2\text{SO}_4$ ) and rinsing thoroughly, the electrode is covered by high valency Os precursors that must be electrochemically reduced to metallic Os islands to display the desired surface catalytic properties, as confirmed by XPS.<sup>12</sup> Assuming that similar aqua-complexes are formed by  $\text{OsCl}_3$  in water to the  $\text{RuCl}_3$  case<sup>14</sup> (the relevant literature data were available for ruthenium<sup>24</sup> but not osmium complexes), a proposed spontaneous deposition mechanism is as follows in the presence of  $\text{O}_2$ :



where  $x$  is a fractional value less than 1 and the osmium in the osmium oxide has a valence between 4 and 8. XPS data indicate that the osmium valence is higher than for  $\text{OsO}_2$ ,<sup>12</sup> but because  $\text{OsO}_4$  has a high vapor pressure, it is not likely the resulting oxide. Therefore, a substoichiometric, perhaps hydroxylated or hydrated osmium oxide form exists on the surface immediately after spontaneous deposition (with no electrochemical actions). The presence of oxygen is required for the deposition of multiple layers of osmium on the surface, although some spontaneous deposition occurs in deaerated solutions, presumably due to reaction of the osmium complexes with the Pt–OH moieties on the surface instead of molecular oxygen. After the spontaneous deposition of the highly oxidized osmium precursors, an electrochemical reduction follows to prepare metallic osmium deposits, as discussed below.

Figure 1a shows a representative cyclic voltammogram for Pt(111)/Os-5min/1mM, indicative of the reduction/stabilization of the Os deposit as a function of the electrode potential.<sup>12</sup> (The term “Pt(111)/Os-5min/1mM” represents a surface prepared by exposing the Pt(111) electrode to a 1 mM  $\text{OsCl}_3 + 0.1 \text{ M H}_2\text{SO}_4$  solution for 5 min, followed by CVs. Below, this notation will be used repeatedly for other time and concentrations to describe the Pt(111)/Os surfaces examined.) The redox couple at 150/200 mV disappears as the high valency Os species are stabilized as the islands of  $\text{Os}(0)$ .<sup>12</sup> Below 300 mV, the features assigned to hydrogen adsorption/desorption become clearly visible. The weak redox couple between 0.6 and 0.8 V is related to the oxidation of metallic Os to  $\text{OsO}_2$ , as previously observed on the polycrystalline Pt/Os<sup>10</sup> and confirmed by XPS and GIF-XAS measurements on Pt(111)/Os.<sup>12</sup> The CV reaches a steady-state after 6–8 scans. The steady-state CVs for Pt(111)/Os surfaces with 0–9 Os packing density (confirmed below) are plotted in Figure 1b–d. The depositions were performed from 5 s to 20 min from the 0.1 mM Os-containing solution as shown in Figure 1b and from 5 s to 6 h in 1 mM Os-containing solution, as shown in Figure 1c,d. For the Pt(111)/Os surfaces prepared by osmium deposition from 0.1 mM Os-containing solution or by up to 10 min deposition from 1 mM Os-containing solution (i.e., up to  $1.1 \pm 0.1$  Os packing density), the addition of Os to Pt(111) changes the total hydrogen adsorption/desorption charge but slightly. This indicates that the surface roughness has practically not increased. For such Pt(111)/Os surfaces (Figure 1(b–c)), the Os deposit reversibly changes from the fully metallic  $\text{Os}(0)$  at potentials  $\leq 0.50 \text{ V}$  to a mixture of  $\text{Os}(0)/\text{Os(IV)}$  at potentials  $\geq 0.50 \text{ V}$ , as previously observed by XPS.<sup>12</sup>

In contrast, prolonged deposition times of 30 min to 6 h in 1 mM  $\text{OsCl}_3 + 0.1 \text{ M H}_2\text{SO}_4$  (Figure 1d) cause a significant increase

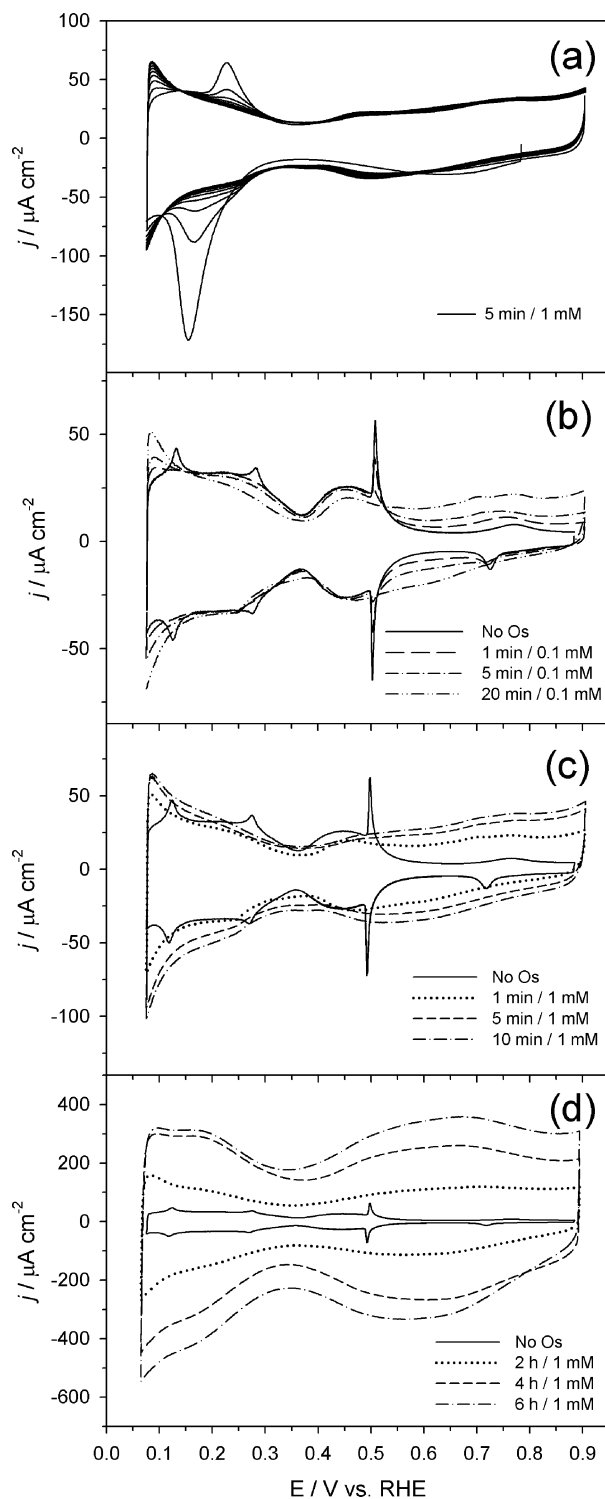


**Figure 1.** Cyclic voltammograms taken in 0.1 M  $\text{H}_2\text{SO}_4$  of a Pt(111) electrode decorated with osmium by spontaneous deposition. The exposure time to (0.1 or 1 mM)  $\text{OsCl}_3 + 0.1 \text{ M H}_2\text{SO}_4$  solution is indicated in the legends. The electrochemical reduction and stabilization of Os species achieved by 8 cycles (up to the steady-state CV) is shown in panel a. The steady-state CVs of Pt(111)/Os surfaces with varying Os coverage are shown in panels b–d: (b) after deposition from 0.1 mM  $\text{OsCl}_3 + 0.1 \text{ M H}_2\text{SO}_4$  solution for 10 s – 20 min; (c) after deposition from 1 mM  $\text{OsCl}_3 + 0.1 \text{ M H}_2\text{SO}_4$  solution for 1–20 min; and (d) 2–6 h. Scan rate,  $50 \text{ mV s}^{-1}$ .

in the pseudocapacitive CV currents. Such an increase can be caused by (1) an increased electroactive surface area related to Os deposition and/or (2) the presence of excessive amounts of the Os oxides/hydroxides that are generated at long deposition

(24) Seddon, E. A.; Seddon, K. R. *The Chemistry of Ruthenium*; Elsevier: New York, 1984; p 1373.

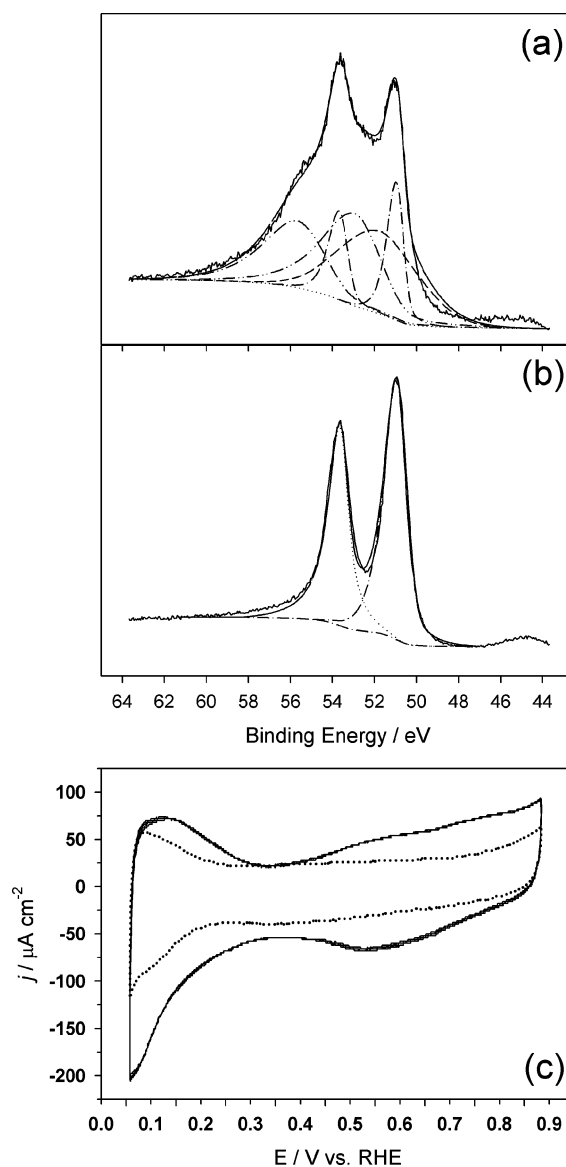


times (note that oxygen is present in the deposition solutions). In the latter case, the pseudocapacitive current results most likely from the  $1\text{ e}^-$  reversible conversion of  $\text{Os}-\text{O}^{2-}$  to  $\text{Os}-\text{OH}^-$ , as previously noted for Pt/Ru.<sup>18,25</sup> To distinguish between the two factors from above, the Pt(111)/Os-2h/1mM electrode was polarized at  $-70\text{ mV}$  for 30 min to reduce the Os oxides/hydroxides produced by spontaneous deposition to metallic Os(0). Milder electrochemically reducing conditions such as holding the potential at  $50\text{ mV}$  for 1 h were not effective for completely reducing multiple layers of osmium to metallic osmium, but rather hydrogen evolution had to occur simultaneously (e.g., at  $-70\text{ mV}$ ) to provide sufficiently reducing conditions. Indeed, after the polarization at  $-70\text{ mV}$ , the CV profiles “collapse”, as shown in Figure 2c. Clearly, the outer Os layer of the multilayer Pt(111)/Os-2h/1mM structure had hindered the reduction of the inner part of the Os deposit to metallic Os in the potential region investigated by cyclic voltammetry above ( $0.07\text{--}0.87\text{ V}$ ).<sup>12</sup>

We have also observed that, after the Os deposits were reduced to Os metal, the original pseudocapacitive appearance of the CV cannot be restored by electrochemical oxidation. That is, the Os oxides/hydroxides obtained from spontaneous deposition, once removed, cannot be formed from metallic Os by simple electrooxidation tactics. However, if the potential step to  $-70\text{ mV}$  is avoided, the Os hydroxides/oxides are stable between  $0.0$  and  $0.9\text{ V}$  for many hours of cycling in pure solution and upon methanol electrooxidation cycles. Although the Os oxides are indeed stable, the  $-70\text{ mV}$  polarization step was applied to all surfaces used for the CO oxidation and methanol oxidation experiments to have a consistent initial Os oxidation state of Os(0).

The presence of Os oxides/hydroxides following spontaneous deposition for prolonged deposition times (30 min to 6 h) as indicated by the CVs was confirmed by XPS data. Figure 2a shows XPS spectra for Pt(111)/Os-30min/1mM after emersion at  $0.5\text{ V}$  after the CVs. The spectra were fit with Os(0) 4f and  $\text{OsO}_2$  4f peaks shown by the dash–dotted and dash–dot–dotted lines, respectively. As in the previous work,<sup>12</sup> peaks at  $50.8 \pm 0.1$  and  $53.5 \pm 0.1\text{ eV}$  are assigned to the Os 4f<sub>7/2</sub> and 4f<sub>5/2</sub> doublet of Os(0), and the peaks at  $51.5 \pm 0.1$  and  $54.2 \pm 0.1\text{ eV}$  correspond to the Os 4f<sub>7/2</sub> and 4f<sub>5/2</sub> doublet of  $\text{OsO}_2$  (Os(IV)). The broad peak at  $52.1 \pm 0.1\text{ eV}$  is assigned to Pt 5p<sub>3/2</sub>. The assignments were made by referring to the spectra of standards of osmium metal,  $\text{OsO}_2$ , and platinum and including a third component for  $\text{OsO}_4$  that could not be directly measured due to the high vapor pressure.<sup>12</sup> See ref 12 for further procedural details. When the area of the peaks corresponding to Os(IV) at  $51.5 \pm 0.1$  and  $54.2 \pm 0.1\text{ eV}$  is compared to the area of the peaks corresponding to Os(0) at  $50.8 \pm 0.1$  and  $53.5 \pm 0.1\text{ eV}$  for Pt(111)/Os-30min/1mM (Os packing density = 1.5), it is clear that the major part (70%) of the Os deposit exists as oxides. This is in a sharp contrast to surfaces with lower Os coverage, for example Pt(111)/Os-5min/1mM (Os packing density = 1), for which the Os deposit is fully metallic and shows no evidence of oxides by XPS after emersion at  $0.5\text{ V}$  (after the same set of CVs).<sup>12</sup> This confirms that the Pt(111) surfaces with very high osmium coverage (several monolayers) resist the reduction of the osmium oxides to osmium metal, as speculated above using cyclic voltammetry.

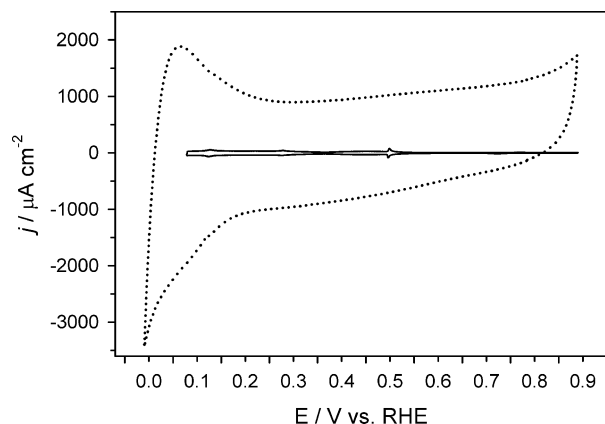
XPS spectra were also collected to confirm that the application of the  $-70\text{ mV}$  potential step described above that causes the CVs to “collapse” reduces these “resistant” Os oxides to the metallic state. This can be clearly seen in the XPS spectra in



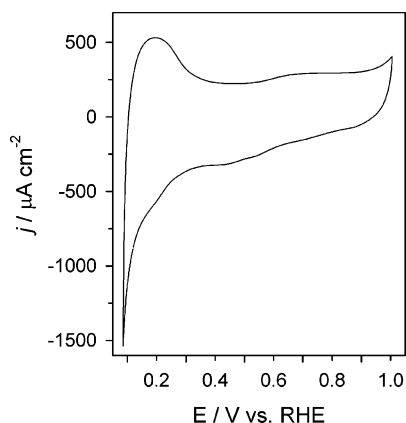
**Figure 2.** Os 4f XPS spectra of osmium spontaneously deposited on Pt(111). As in the previous work,<sup>12</sup> peaks at  $50.8 \pm 0.1$  and  $53.5 \pm 0.1\text{ eV}$  are assigned to the Os 4f<sub>7/2</sub> and 4f<sub>5/2</sub> doublet of Os(0), and the peaks at  $51.5 \pm 0.1$  and  $54.2 \pm 0.1\text{ eV}$  correspond to the Os 4f<sub>7/2</sub> and 4f<sub>5/2</sub> doublet of  $\text{OsO}_2$  (Os(IV)). The broad peak at  $52.1 \pm 0.1\text{ eV}$  is assigned to Pt 5p<sub>3/2</sub>. (a) Pt(111)/Os-30min/1mM, with Os oxides predominating; (b) Pt(111)/Os-2h/1mM, after electrode polarization at  $-70\text{ mV}$  for 30 min to reduce Os oxides to metallic Os(0); (c) CVs showing how the reduction of Os oxides present on Pt(111)/Os-2h/1mM (solid line) to the purely metallic Os state (dotted line) is clearly observed by the change in the CV characteristics.

Figure 2b for Pt(111)/Os-2h/1mM (Os packing density = 3) as the Os oxide peaks are completely missing. Thus, the oxides present after a prolonged osmium deposition (30 min to 2 h from 1 mM Os solution) can be fully reduced to the metallic Os state with a 30 min,  $-70\text{ mV}$  potential step. XPS data for Pt(111)/Os prepared by longer deposition times than 2 h were not collected, but similar changes in oxidation state can be inferred from the corresponding changes in the CVs, as demonstrated in Figure 2c. For all of the Pt(111)/Os surfaces in this report, the  $-70\text{ mV}$  potential step was applied and a fully reduced, metallic Os deposit was present on the initial surface.

As a control experiment, approximately 50 layers of Os were electrodeposited on Pt(111) from 1 mM  $\text{OsCl}_3 + 0.1\text{ M H}_2\text{SO}_4$  at  $40\text{ mV}$ , and a typical CV curve is presented in Figure 3. Here,



**Figure 3.** Cyclic voltammogram (dotted line) in 0.1 M H<sub>2</sub>SO<sub>4</sub> of Os electrodeposits (≈50 layers) on Pt(111) prepared by polarization at 40 mV in 1 mM OsCl<sub>3</sub> + 0.1 M H<sub>2</sub>SO<sub>4</sub> solution. The current density is referenced to the geometric Pt(111) area. The cyclic voltammogram of the clean Pt(111) electrode is shown as a solid line to demonstrate the scale.



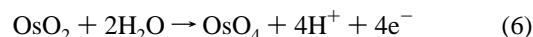
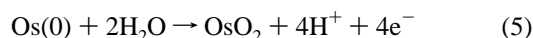
**Figure 4.** Cyclic voltammogram of an Os ingot in 2.0 M H<sub>2</sub>SO<sub>4</sub>, after polarization at 0.0 mV for 5 min to ensure a metallic Os. Sweep rate, 10 mV/s. Potential is reported vs RHE for 0.1 M H<sub>2</sub>SO<sub>4</sub>, not 2.0 M H<sub>2</sub>SO<sub>4</sub>.

the amount of Os deposit was estimated from the Os stripping voltammetry (as described in section 3.2), and the current densities are reported versus the geometric electrode surface area. The CV figure shows hydrogen adsorption/desorption in the range 0.0–0.25 V, as well as the threshold of a significant Os oxidation at 0.8 V. The CV is similar to that observed for Os electrodeposited on a Pt foil<sup>26</sup> and compares well to that of the bulk Os ingot (Experimental Section), as reported below.

Voltammetric experiments on the bulk Os ingot were performed at 10 mV/s (Figure 4). A higher concentration of sulfuric acid was used to highlight the key specific voltammetric features of the electrode. A cathodic pretreatment was implemented at –50 mV for 5 min to ensure a fully metallic Os surface. The surface area is uncertain and currents are normalized to the geometric surface area. The main CV features are similar to those presented in Figure 1a for the Pt(111)/Os-min/1mM, noting the potential shift due to the higher solution pH. The hydrogen region extends from 0.1 to 0.35 V, and the broad oxidation/reduction couple due to the oxidation of Os(0) to OsO<sub>2</sub> is centered at ca. 0.55 V.

**3.2. Os Stripping Voltammetry.** Oxidative dissolution of Os (the Os stripping) was performed to quantify the charge needed to remove the Os deposit from the Pt(111) surface and the amount of Os on the surface (the Os packing density). Data in Figure

5a show the first four electrodisolution cycles for Pt(111)/Os-2h/1mM. The CV peak associated with the removal of Os as OsO<sub>4</sub><sup>12</sup> appears near 1.15 V. After the first sweep, only a small fraction of the original osmium deposit remains on the surface, which is completely removed in the remaining sweeps. Figure 5b shows the only first sweep (for clarity) for several Pt(111)/Os surfaces with different Os coverage values. To calculate the Os packing density, the charge at the peak of 1.15 V from the first three sweeps was divided by the number of electrons engaged in the Os oxidation (*n*). However, the *n* value depends on the oxidation state of surface Os at the threshold of dissolution, and was obtained using the following reactions:<sup>27</sup>



The Os oxidation state just prior to the Os stripping peak was determined using XPS results, see also ref.<sup>12</sup> For the low to moderate Os coverage, ca. 20% Os(0) and ca. 80% Os(IV) exist on Pt(111)/Os just before the stripping peak. This gives an average *n* value equal to 4.8 e<sup>–</sup> per Os atom. In contrast, the value of *n* = 8 e<sup>–</sup> per a metallic Os atom is adequate to calculate the amount of Os for ≥ 30 min/1 mM deposition. As discussed above, the multiple monolayers of osmium deposit obtained with prolonged deposition times were resistant to a complete reduction to osmium metal, and the converse is also true, that the multiple layers of osmium are resistant to oxidation during the course of a single linear potential sweep. Using the value *n* = 8 e<sup>–</sup> may result in a slightly underestimated Os coverage, which is negligible for the multiple layers of the Os deposits.

The Os packing density for each Pt(111)/Os surface was thus calculated by dividing the total Os stripping charge (e.g., Figure 5a) by the estimated value of *n* as described above. These calculated Os packing densities<sup>28</sup> are shown in Table 1. The table (and Figure 5c,d) demonstrates that, as the osmium deposition time increases, the Os packing density also increases. For example, exposing Pt(111) to the 1 mM Os-containing solution for 5 min gives a packing density of ≈1, whereas an exposure time of 6 h gives a packing density of ≈9. Table 1 also demonstrates the effect of the Os-solution concentration on the amount of deposit obtained. An exposure of Pt(111) for 1 min to the 0.1 mM Os solution gives a packing density of ≈0.3, compared to the osmium packing density of 0.8 obtained from a 1 min exposure to the 1 mM Os solution. The Os coverage estimates calculated from the Os stripping are in good agreement with the estimates based on the XPS data. For example, the XPS Os<sub>4f</sub>/Pt<sub>4f</sub> peak ratio of 1.09 for Pt(111)/Os-2h/1mM corresponds to 2.8 layers of Os based on a standard XPS intensity ratio equation.<sup>29</sup> Thus, the estimate of 2.8 ± 0.2 Os packing density from the Os stripping voltammetry is in a very good agreement with the XPS results.

**3.3. Pt(111)/Os in Situ STM Images.** To reveal the structural details of the Os deposit on Pt(111), in situ STM images were obtained for Pt(111)/Os-1min/0.1mM, Pt(111)/Os-1min/1mM, and Pt(111)/Os-5min/1mM. After using the I<sup>–</sup>/CO procedure to obtain the clean Pt(111) surface as previously reported (adsorbing I<sup>–</sup> from 1 mM KI solution, displacing adsorbed iodine layer with

(27) Zoubov, N. D.; Pourbaix, M. In *Atlas of Electrochemical Equilibria in Aqueous Solutions*; Pourbaix, M., Ed.; National Association of Corrosion Engineers: Houston, 1974; p 235.

(28) Waszczuk, P.; Solla-Gullon, J.; Kim, H. S.; Tong, Y. Y.; Montiel, V.; Aldaz, A.; Wieckowski, A. *J. Catal.* **2001**, 203 (1), 1–6.

(29) Watts, J. F. *An Introduction to Surface Analysis by XPS and AES*; John Wiley and Sons: New York, 2003; p 224.

(26) Peinado, J.; Colom, F. *Anal. Quim.* **1978**, 74 (3), 390–397.

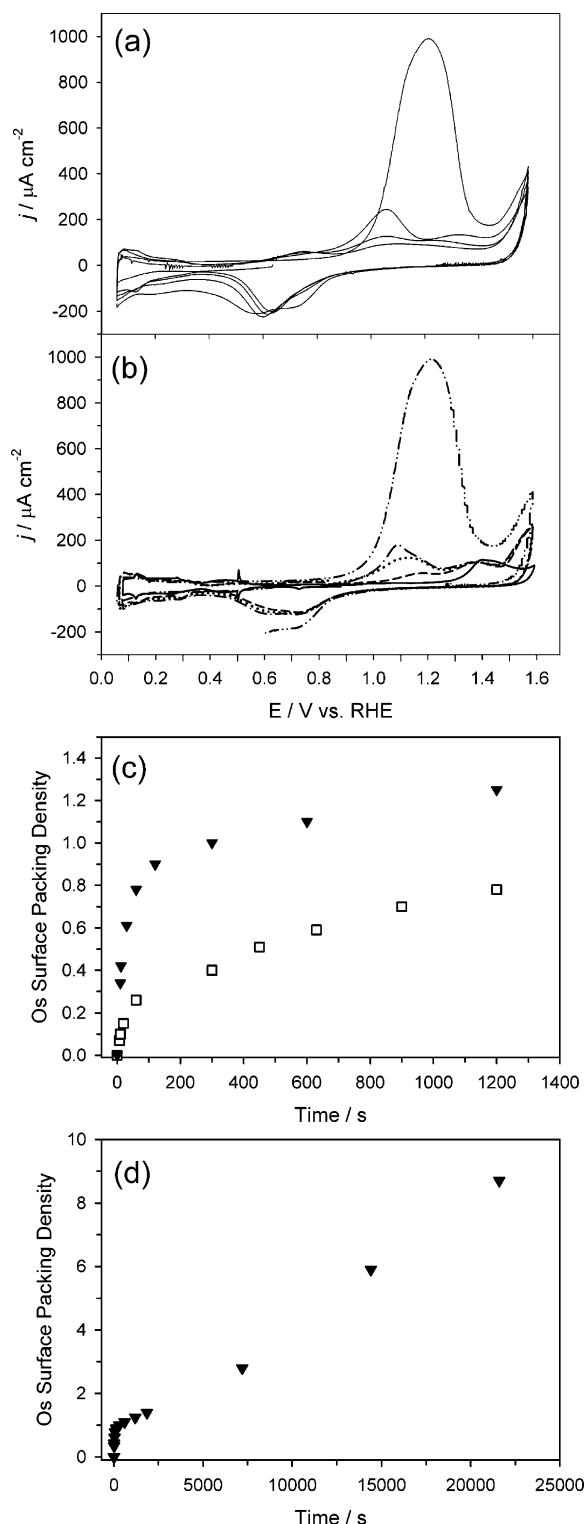


**Figure 5.** (a) Cyclic voltammograms (4 cycles) taken in 0.1 M  $\text{H}_2\text{SO}_4$  of a Pt(111)/Os-2h/1mM electrode showing the electrochemical oxidation (stripping) of Os to  $\text{OsO}_4$ , scan rate,  $10 \text{ mV s}^{-1}$  (b) the first cycle as in panel a for Pt(111) surfaces with different Os coverage: clean Pt(111) (solid line), Pt(111)/Os-1min/0.1mM (dashed line), Pt(111)/Os-1min/1mM (dotted line), Pt(111)/Os-5min/1mM (dash-dotted line), and Pt(111)/Os-2h/1mM (dash-dot-dotted line). (c) Plot showing the increase in Os packing density (as calculated from the charge of Os stripping) with exposure time to (0.1 or 1 mM)  $\text{OsCl}_3 + 0.1 \text{ M H}_2\text{SO}_4$  solution: 0.1 mM  $\text{OsCl}_3 + 0.1 \text{ M H}_2\text{SO}_4$  (open squares), and 1 mM  $\text{OsCl}_3 + 0.1 \text{ M H}_2\text{SO}_4$  (filled triangles) up to 1200 s (20 min) deposition time. (d) Same as part c, for deposition time up to 21,600 s (6 h) from 1 mM  $\text{OsCl}_3 + 0.1 \text{ M H}_2\text{SO}_4$ .

**Table 1. Os Packing Density on Pt(111)/Os Surfaces Calculated Using the Charge under the Os Electrooxidation Peaks (See Figure 2 and Text)<sup>a</sup>**

deposition conditions	Os packing density
surfaces with 0–1.1 Os packing density	calculated using $\approx 20\%$ $\text{Os(0)} \rightarrow 80\% \text{ Os(IV)} \rightarrow \text{Os(VIII)}$ $n = 4.8 e^-$ (average) (based on XPS data <sup>12</sup> )
10 s/0.10 mM	$0.10 \pm 0.02$
1.0 min/0.10 mM	$0.28 \pm 0.04$
1.0 min/1.0 mM	$0.78 \pm 0.07$
5.0 min/1.0 mM	$1.0 \pm 0.1$
10.0 min/1.0 mM	$1.1 \pm 0.1$
surfaces with $\gg 1$ Os packing density	calculated using $\text{Os(0)} \rightarrow \text{Os(VIII)}$ $n = 8 e^-$ (based on XPS data, in text)
2.0 h/1.0 mM	$2.8 \pm 0.2$
4.0 h/1.0 mM	$6.0 \pm 0.5$
6.0 h/1.0 mM	$9 \pm 1$

<sup>a</sup> Pt(111)/Os surfaces were prepared by spontaneous deposition from (0.1–1.0) mM  $\text{OsCl}_3 + 0.1 \text{ M H}_2\text{SO}_4$ .

$\text{CO}$ , then electrochemically oxidizing  $\text{CO}$ ),<sup>13</sup> Os was deposited on the surface by spontaneous deposition directly in the STM cell. STM images of osmium in the metallic state<sup>12</sup> at 0.1 V were then obtained. Presented in Figure 6a is an image of Pt(111)/Os-1min/0.1mM at the Os coverage of  $0.22 \pm 0.05 \text{ ML}$ . The percentages of Os islands having heights of 1–4 atomic layers (taking each Os atomic layer as ca. 0.23 nm high) are depicted in a histogram in Figure 6b. Of the islands,  $50 \pm 5\%$  have only one Os layer. Although about 50% of the islands have more than one Os layer, the multilayer part of the island is generally located in the center of the island and does not extend to the island edge (even after considering tip broadening effects). Thus, for the Os islands on Pt(111), the actual surface area covered by multilayer growth is not accurately reflected by only counting the islands with multilayer height. To address this issue, the multilayer growth was calculated in terms of surface area coverage. As shown in the histogram in Figure 6c, about 0.15 ML of the Os deposit is only 1 atomic layer high. That is, about 70% (0.15 ML/0.22 ML total) of the Os deposit area is only of monatomic height. In short, although about 50% of the islands have some multilayer growth, only about 30% of the osmium island area has multilayer height due to the nonuniform height of the individual islands (i.e., a “two layer island” is generally only one layer high around the perimeter).

The image of Pt(111)/Os-1min/1mM in Figure 7a1 shows much higher coverage ( $0.6 \pm 0.1 \text{ ML}$ ). However, the island height distributions and island widths are quite similar to Pt(111)/Os-1min/0.1mM. Again, about half of the islands have multiple layers, as shown by the histogram in Figure 7a2. Of the Os deposit, about 0.4 ML is only 1 atomic layer high, as shown in the histogram in Figure 7a3. This fraction of monatomic growth is consistent with the previous case, since (0.4 ML/0.6 ML total) equals about 70% of the Os deposit area. As before, the islands have predominantly 1–3 nm widths. The island density increases from  $\approx 5 \times 10^{10}$  islands/ $\text{cm}^2$  for Pt(111)/Os-1min/0.1mM to  $\approx 1.5 \times 10^{11}$  islands/ $\text{cm}^2$  for Pt(111)/Os-1min/1mM. Finally, the STM image of Pt(111)/Os-5min/1mM is shown in Figure 7b1. Here, the area coverage of osmium increases further to  $0.7 \pm 0.1 \text{ ML}$ . Again, the island height distributions (Figure 7b2) and the island widths (1–3 nm) show little change. The island density has further increased to  $\approx 2 \times 10^{11}$  islands/ $\text{cm}^2$ . Based on this osmium island growth pattern, the increase in the amount of osmium deposit directly correlates to an increase in Pt–Os border sites, at least until the platinum sites begin to be obscured by osmium.



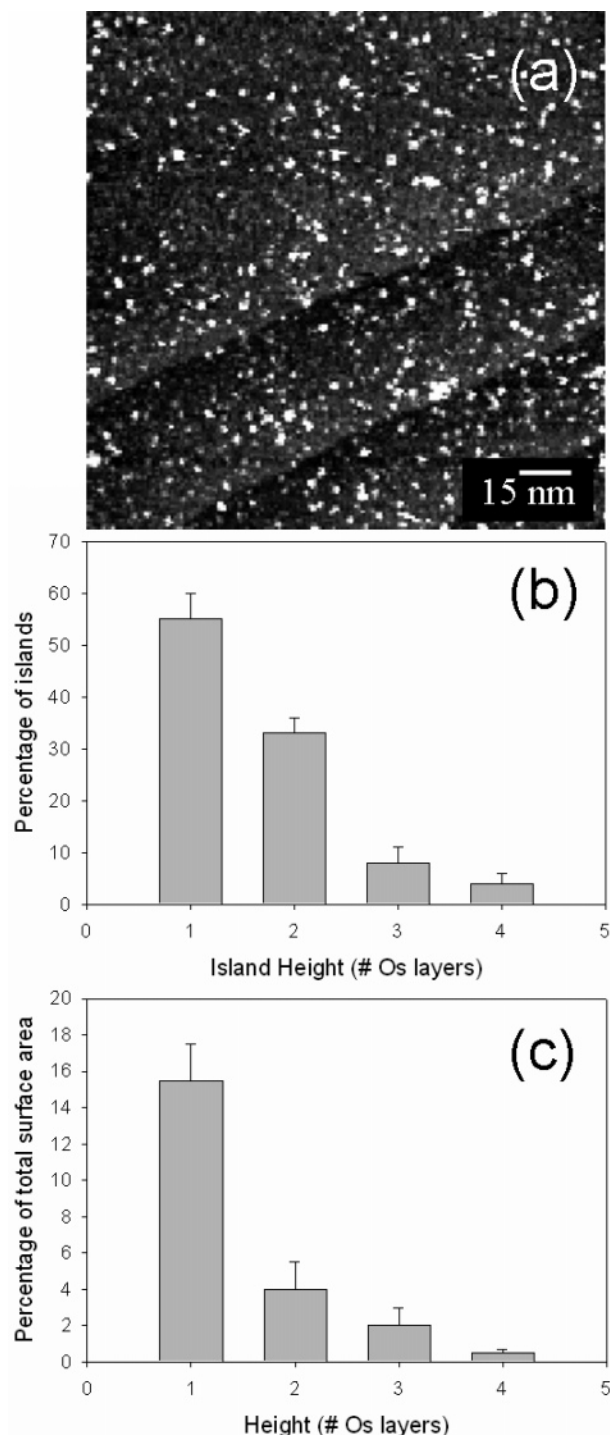


**Figure 6.** (a) In situ STM image (150 nm  $\times$  150 nm) of Os-modified Pt(111) recorded at 0.1 V in 0.1 M  $\text{H}_2\text{SO}_4$  after Os was deposited from 0.1 mM  $\text{OsCl}_3$  in 0.1 M  $\text{H}_2\text{SO}_4$  for 1 min; (b) a chart showing the height distribution of the osmium islands; (c) a chart showing the percent coverage of the Pt(111) surface by Os layers.

The image of a Pt(111)/Os surface with very high Os-coverage, Pt(111)/Os-1h/1mM, is shown in Figure 8. The image was obtained after reducing the Os deposit fully to Os(0) by holding the potential at  $-70$  mV for 30 min. Most of the islands are still 1–3 nm wide, but now there are more 3.5–5 nm islands. It was difficult to determine a background with such high coverage (ca. 3 Os packing density, and see Figure 8), so the island height distribution and the Os coverage value were not determined. Certainly, fewer than 10% of the original Pt sites remain.

**3.4. Carbon Monoxide Stripping Voltammetry.** Figure 9 shows the CO stripping voltammogram from Pt(111)/Os surfaces in the CO-free solution (following dosing in the CO-saturated solution). If the Pt(111)/Os-10s/1mM surface is used (Figure 9a, solid line), the hydrogen region is fully suppressed, and two overlapping CO stripping peaks are observed at 0.57 and 0.62 V.<sup>13</sup> It was previously concluded for Pt(111)/Ru–CO<sup>13,30</sup> that the first peak originates from CO removal on and perhaps proximal to the edge of the Ru islands. We believe that this pattern also prevails for Pt(111)/Os–CO.<sup>13</sup> The second peak originates, by analogy, from the oxidation of CO from Pt(111) sites farther away from the Os islands. For Pt(111)/Os-5min/1mM, only one CO stripping peak is observed (at 0.53 V) with a pronounced tailing. The second peak has diminished because the Os coverage increased from  $0.22 \pm 0.05$  to  $0.7 \pm 0.1$  (from STM, see above), leaving only a small fraction of Pt sites far from the Os island edge. The more negative onset potential and peak potential for CO oxidation on Pt(111)/Os-5min/1mM are notable, since these shifts correlate to the improved methanol electrooxidation performance that is discussed in the next section. The CO stripping curves for Pt(111)/Os-2h/1mM (dotted line) and Pt(111)/Os-6h/1mM (dash–dotted line) show the current due to CO removal from additional Os sites over a broad potential range up to 0.9 V.

The CO stripping curves also provide an estimate of the real electroactive surface area of the Pt(111)/Os electrodes. The CO coverage increases from  $0.70 \pm 0.05$  ML for the clean Pt(111) surface to  $0.80 \pm 0.05$  ML for Pt(111)/Os-10s/1mM. On Pt(111)/Os-5min/1mM, the coverage value is  $0.9 \pm 0.1$  ML. The CO coverage further increases to  $1.2 \pm 0.2$  ML for Pt(111)/Os-2h/1mM and  $1.8 \pm 0.3$  ML for Pt(111)/Os-6h/1mM. (The CO coverage was calculated from the CO stripping charge compared to the electroactive area<sup>31</sup> of the Pt(111) electrode =  $0.25 \text{ cm}^2$ .) The real electroactive surface area clearly increases with the added Os, which must be considered when reviewing the methanol electrooxidation results.

We note that the CO adsorption and oxidation process irreversibly changes the Pt(111)/Os surfaces, perhaps through an electrochemical annealing process that rearranges the Os deposit to cover more Pt sites.<sup>32</sup> If the CO stripping experiment is repeated as shown in Figure 9b, the CO stripping peak is broadened and shifted to the right by about 30 mV, indicating that the surface was changed by the previous experiment. The peak area is slightly smaller, indicating that some residual CO remains or surface area was lost. The effect cannot be reversed by positive or negative potential steps. Additionally, Pt(111)/Os surfaces are less active to methanol electrooxidation after the prior exposure to CO gas (not shown).

**3.5. Methanol Electrooxidation Chronoamperometry and General Comparisons to Pt(111)/Ru.** As mentioned in the Introduction, the methanol electrooxidation data presented below can be analyzed assuming that a bifunctional mechanism is operating, whereby the platinum sites serve to chemisorb methanol and the osmium sites provide oxygen-species (e.g., OH) in sufficient numbers to completely oxidize the CO produced by methanol decomposition. As formulated previously for Pt/Ru

(30) Lu, G. Q.; Waszczuk, P.; Wieckowski, A. *J. Electroanal. Chem.* **2002**, 532 (1–2 Special Issue SI), 49–55.

(31) Clavilier, J. In *Interfacial Electrochemistry: Theory, Experiment, and Applications*; Wieckowski, A., Ed.; Marcel Dekker: New York, 1999; pp 231–267.

(32) Lin, W. F.; Iwasita, T.; Vielstich, W. *J. Phys. Chem. B* **1999**, 103 (16), 3250–3257.

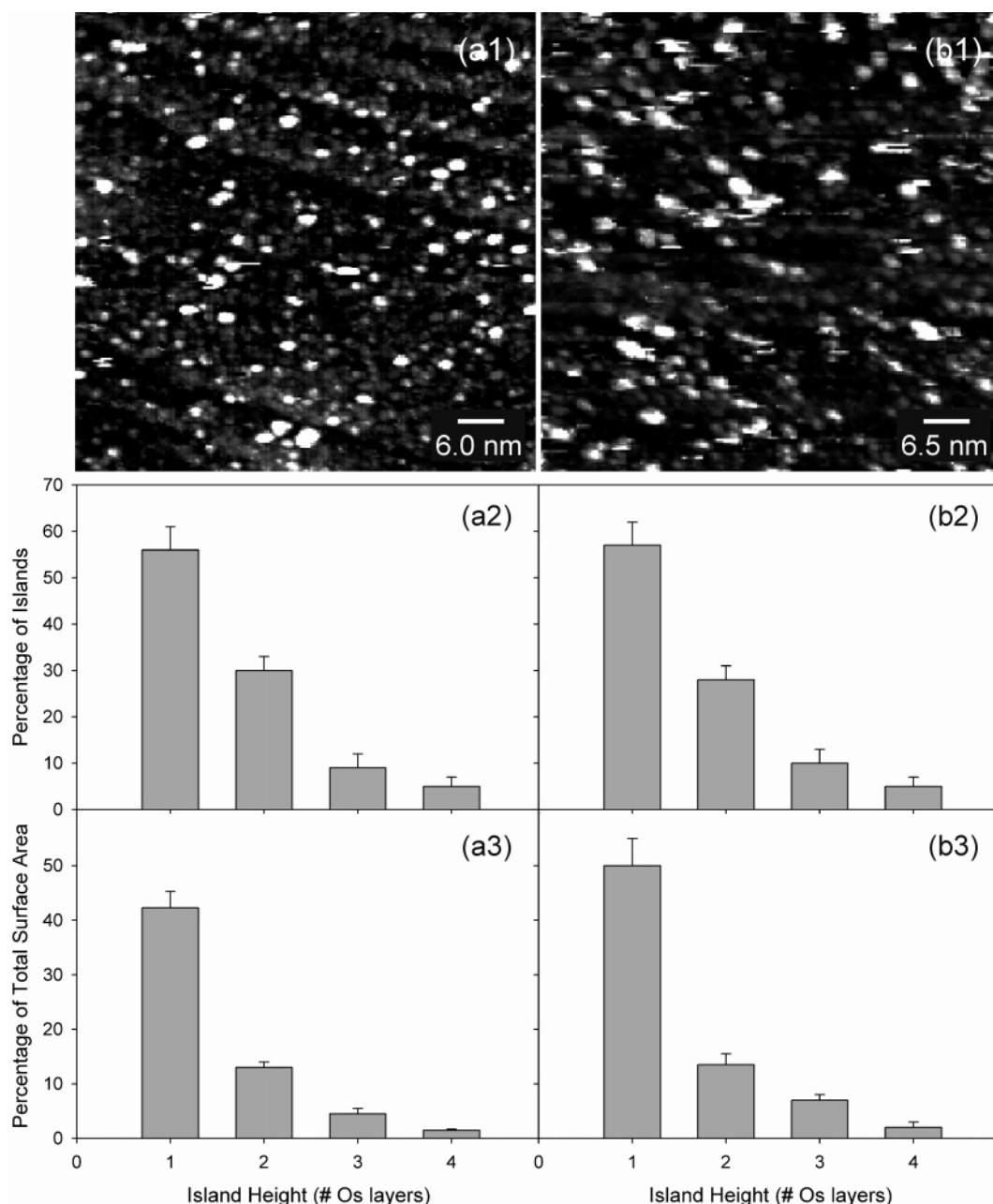


**Figure 7.** In situ STM images of Os-modified Pt(111) recorded at 0.1 V in 0.1 M H<sub>2</sub>SO<sub>4</sub> after Os was spontaneously deposited from 1 mM OsCl<sub>3</sub> in 0.1 M H<sub>2</sub>SO<sub>4</sub> for: (a1) 1 min (60 nm × 60 nm) and (b1) 5 min (60 nm × 60 nm). Charts follow showing the height distribution of the osmium islands (a2 and b2), as well as the percent coverage of the Pt(111) surface by Os layers (a3 and b3).

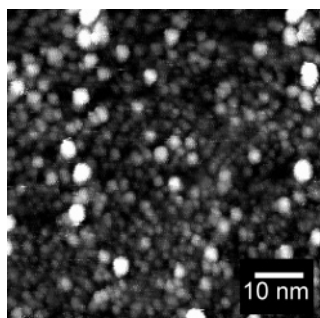
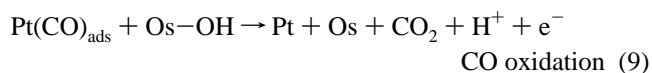
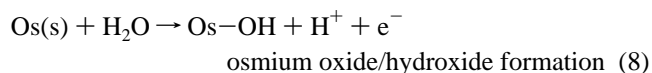
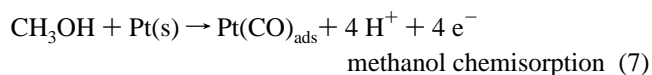


**Figure 8.** In situ STM image of Os-modified Pt(111) (65 nm × 65 nm) recorded at 0.1 V in 0.1 M H<sub>2</sub>SO<sub>4</sub> after Os was spontaneously deposited from 1 mM OsCl<sub>3</sub> in 0.1 M H<sub>2</sub>SO<sub>4</sub> for 1 h. The image was taken after polarization at −70 mV for 30 min.

surfaces,<sup>3,16,33</sup> the bifunctional mechanism as it applies to methanol oxidation on Pt(111)/Os can be summarized in the following

processes (elementary steps are not specified):



Here, Os–OH means any oxide/hydroxide form of osmium, the exact nature of which is irrelevant for the following discussion. The total rate of process (7) depends on the number of Pt sites

(33) Watanabe, M.; Vehida, M.; Motoo, S. *J. Electroanal. Chem.* **1987**, 229, 395–406.



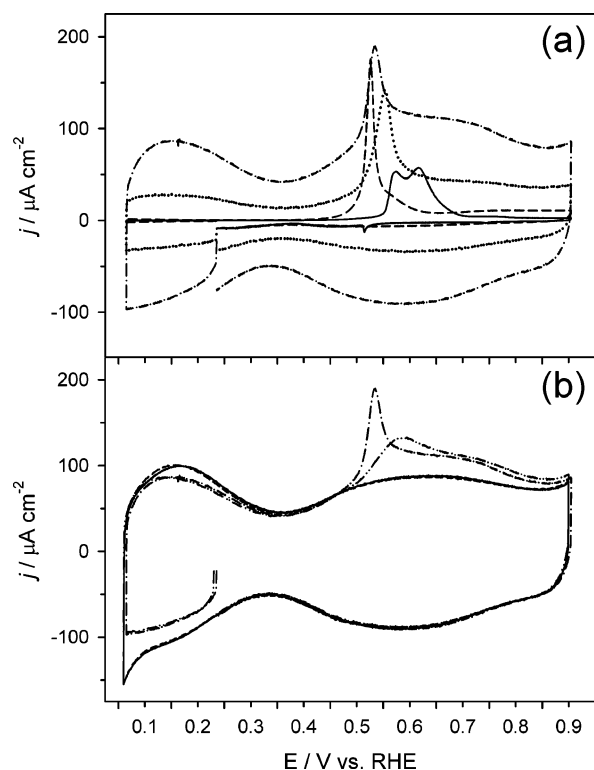


**Figure 9.** Voltammograms in 0.1 M  $\text{H}_2\text{SO}_4$  showing oxidative removal of CO from Pt(111)/Os surfaces (CO stripping) as the potential is swept positively. CO was bubbled for 10 min at 0.20 V, followed by 5 min of Ar bubbling. CO stripping voltammograms were obtained for the following surfaces: Pt(111)/Os-10s/1mM (solid line) and Pt(111)/Os-5min/1mM (dashed line), Pt(111)/Os-2h/1mM (dotted line), and Pt(111)/Os-6h/1mM (dash-dotted line). Sweep rate, 10 mV/s.

available, whereas the overall rate of process (8) depends on the number of Os sites, and perhaps only the number of Pt–Os border sites if the Os–OH species is not highly mobile. The overall rate of process (9) depends only on the number of Pt–Os border sites. These points will be used in the discussion of the methanol electrooxidation data below.

Measurements of the methanol electrooxidation rates on Pt(111)/Os surfaces were performed by chronoamperometry at 0.40, 0.50, and 0.55 V in 0.6 M  $\text{CH}_3\text{OH}$  + 0.1 M  $\text{H}_2\text{SO}_4$  solution. After characterizing the Os deposits by CV, as in Figure 1, and holding the potential at  $-70$  mV to reduce any Os oxides to the metallic state, the Pt(111)/Os electrode was transferred to another electrochemical cell containing the methanol solution. In Figure 10, methanol electrooxidation results are plotted versus Os packing density rather than versus the Os coverage so that all of the data can be displayed together (STM data are not available for every point). For each measurement, the electrode potential was held at 50 mV as the electrode was immersed in the methanol solution before stepping the potential positively to initiate the methanol oxidation.

Figure 10a1 shows selected chronoamperometric current density–time transients at 0.40 V. The current densities are quoted versus the Pt(111) electroactive area ( $0.25 \text{ cm}^2$ ) prior to osmium deposition. Figure 10a2 demonstrates the increase in the oxidation current density with Os packing density (up to  $1.0 \pm 0.1$  (Pt(111)/Os-5min/1mM)) and then decreases for  $1.1 \pm 0.1$  packing density (Pt(111)/Os-10min/1mM). The optimal osmium surface coverage, as given by the STM measurements, is  $0.7 \pm 0.1$  ML. Apparently, the Pt(111)/Os surface requires many osmium sites for processes (8 and 9) to achieve the fastest overall methanol decomposition rate, suggesting that one of these processes is

rate-limiting. Indeed, the negative shift in the onset potential for CO oxidation as osmium coverage increases shown in the previous section demonstrates the improvement in the rate of one of these processes. However, when too many Pt sites are covered by Os, the methanol activity decreases because of the severely reduced number of Pt sites for methanol chemisorption as depicted in process 7.<sup>1</sup>

Figure 10b1,b2 demonstrates a similar trend at 0.50 V, with the maximal activity again occurring at  $1.0 \pm 0.1$  packing density (Pt(111)/Os-5min/1mM). The same behavior is confirmed for 0.55 V (Figure 10c1,c2). For the 0.55 V data, the Pt(111)/Os surfaces were prepared using 0.1 mM Os-containing solution to generate a low Os coverage, yet the methanol oxidation current maximum was still at  $1.0 \pm 0.1$  Os packing density. Over this potential range, the rate of either process 8 or 9 (whichever is limiting) has not increased enough to overcome the need for a high osmium coverage, even though the overall methanol oxidation rate has increased with potential.

Comparing Pt(111)/Os to the island-type Pt(111)/Ru surfaces, the optimal Os coverage,  $0.7 \pm 0.1$  ML, is higher than the optimal Ru coverage (which is in the range of 0.2–0.5 ML).<sup>16,17,28</sup> The differences in chemical properties of these two metals can account for the different optimal coverage values. According to the bifunctional mechanism, ensembles of 2–4 Pt sites<sup>1</sup> are required for the methanol chemisorption that results in the formation of a CO intermediate. These Pt ensembles, however, must border a Ru–OH or Os–OH site (with OH meaning some reactive oxygen-containing species) to efficiently remove CO.<sup>1</sup> We propose that a relatively high coverage of Os on Pt(111) is needed to supply a sufficient number of Os–OH sites, given that osmium is less oxophilic under our electrochemical conditions than ruthenium, e.g., based on XPS results. For example, only about 20% of the Os deposit is oxidized at 0.6 V,<sup>12</sup> whereas about 60–70% of the Ru deposit is then oxidized under the same conditions.<sup>22</sup> This suggests that process 8, the formation of Os–OH species, is rate-limiting, although a slow reaction of Pt–CO with Os–OH (process 9) cannot be excluded.

A possibility that must be addressed given the high osmium coverage values encountered here is that the osmium itself participates significantly in methanol chemisorption (process 7). Although osmium slowly chemisorbs methanol at room temperature,<sup>34</sup> unlike ruthenium which does not,<sup>35,36</sup> the rate of methanol oxidation on osmium is very slow (see below).<sup>34</sup> This demonstrates that osmium sites cannot play the dominant role in methanol chemisorption. As mentioned above, the XPS data for Pt(111)/Os did not show evidence of charge transfer between Pt and Os,<sup>12</sup> indicating that electronic effects that could enhance this process are small. Therefore, and overall, the electrooxidation of methanol on Pt(111)/Os can be best rationalized by the bifunctional mechanism provided that the differences between the oxophilicity of the Ru and Os deposits under electrochemical conditions are considered.

**3.6. Comparison of the Methanol Electrooxidation Activity of Specific Pt(111)/Os and Pt(111)/Ru Catalysts.** The performance of Pt(111)/Os to Pt(111)/Ru catalysts for methanol electrooxidation at several potentials is compared in Table 2. After 10 min polarization at 0.40 V, Pt(111)/Os performs worse than Pt(111)/Ru, but is about the same at 0.50 V and better at 0.55 V. (Note that the activity of Pt(111)/Os at 0.55 V falls below that of Pt(111)/Ru at much longer times (e.g., 2 h), due

(34) Orozco, G.; Gutierrez, C. *J. Electroanal. Chem.* **2000**, 484 (1), 64–72.

(35) Lin, W. F.; Jin, J. M.; Christensen, P. A.; Scott, K. *Electrochim. Acta* **2003**, 48 (25–26), 3815–3822.

(36) Franaszczuk, K.; Sobkowski, J. *J. Electroanal. Chem.* **1992**, 327 (1–2), 235–245.

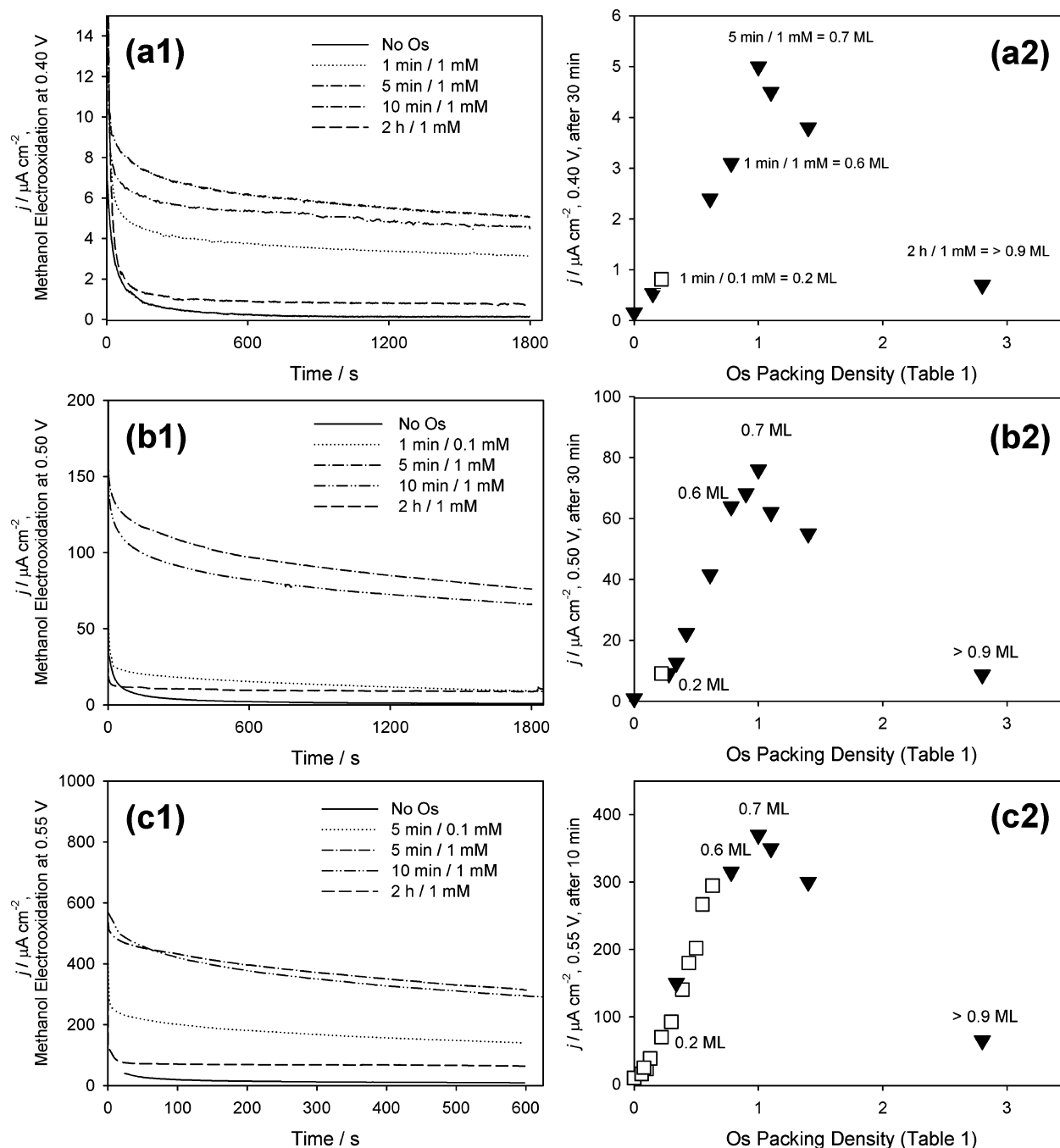


**Figure 10.** Selected methanol electrooxidation current density-vs.-time transients in 0.6 M  $\text{CH}_3\text{OH}$  + 0.1 M  $\text{H}_2\text{SO}_4$  solution for Pt(111)/Os surfaces with electrode potentials of 0.40, 0.50, and 0.55 V vs RHE are shown in panels a1, b1, and c1, respectively. The methanol electrooxidation current densities at 0.40 and 0.50 V at 30 min (with more data points) are plotted versus the Os packing density in panels a2 and b2. The current densities at 0.55 V at 10 min are plotted versus the Os packing density in panel c2. The gray squares represent deposition from 0.1 mM  $\text{OsCl}_3$  + 0.1 M  $\text{H}_2\text{SO}_4$ , and the black triangles represent deposition from 1 mM  $\text{OsCl}_3$  + 0.1 M  $\text{H}_2\text{SO}_4$ . The known surface area coverage values (ML) of Pt(111)/Os determined by in situ STM are written by selected points on the graph. Current density was referenced to the Pt(111) area = 0.25  $\text{cm}^2$ .

**Table 2.** Comparison of Methanol Electrooxidation Current Densities Obtained on Pt(111)/Os and Pt(111)/Ru Surfaces after 10 and 30 min Polarization Time in 0.6 M  $\text{CH}_3\text{OH}$  + 0.1 M  $\text{H}_2\text{SO}_4$  Solution<sup>a</sup>

methanol electrooxidation potential	current after 10 min/ $\mu\text{A cm}^{-2}$		current after 30 min/ $\mu\text{A cm}^{-2}$	
	Pt(111)/Os	Pt(111)/Ru	Pt(111)/Os	Pt(111)/Ru
0.40 V	3.8	$\approx 20$ (ref 17)	2.2	$\approx 10$ (ref 17)
0.50 V	100	$\approx 65$ (ref 42)	75	$\approx 60$ (ref 42)
0.55 V	370	$\approx 100$ –120 (refs 11 and 17)	200	$\approx 80$ –100 (ref 42)

<sup>a</sup> The potentials of the referenced data have been adjusted to RHE as defined here.

to faster deactivation of Pt(111)/Os over time.) The increased activity of Pt(111)/Os at 0.50 and 0.55 V in comparison to the

poor activity at 0.40 V ( $\approx 0\%$  oxides) correlates well with the appearance of Os oxides between 0.50 and 0.60 V ( $\approx 20\%$  oxides),

as determined by XPS.<sup>12</sup> The appearance of more oxidized osmium species correlates to an increase the rates of processes 8 and 9 as discussed above. The optimal osmium coverage has not changed with increasing potential, suggesting that these processes are still slower than the methanol chemisorption process 7. The rate of methanol electrooxidation on Pt(111)/Os is superior to the rates on Pt(111)/Ru at 0.55 V because the ruthenium has become overly oxidized compared to osmium and is no longer in the optimal oxidation state for processes 8 and 9.<sup>22</sup> It is important to emphasize that, over the potential range studied, the osmium deposits have a much lower proportion of oxides than the ruthenium deposits (maximum 20%<sup>12</sup> compared to 60–70%<sup>22</sup>), which results in different optimal coverage values and different behavior with respect to potential.

The decay of the methanol oxidation current on Pt(111)/Os over time, as seen in Figure 10, is even more pronounced compared to the current decays on Pt(111)/Ru surfaces.<sup>15,17,37</sup> For Pt(111)/Os, some current density can be regained by stepping the potential to 75 mV for a few seconds, but more improvement is gained by polarization at 0.90 V which also restores the initial, fast-decaying current transient. Using both potential steps in sequence restores the original current. Explanations that are analogous to those offered by Hoster et al.<sup>37</sup> concerning the causes of current decay on Pt(111)/Ru surfaces may also be relevant here. The potential step to 75 mV may restore the active Os–OH sites by reducing OsO<sub>2</sub> (analogously to RuO<sub>2</sub> on Pt(111)/Ru<sup>37</sup>), and the second potential step to 0.90 V may remove the products of incomplete methanol oxidation (analogously to Pt(111)/Ru<sup>37</sup>). On the time-scale of several hours rather than minutes, such current decays were also observed for Pt–Os alloy nanoparticle catalysts.<sup>38</sup>

**3.7. Reactivity of Os toward Methanol without the Influence of Platinum Substrate.** The reactivity of Os toward methanol oxidation without the influence of the platinum substrate was also investigated to address the possibility of osmium participating extensively in methanol chemisorption.<sup>34,39</sup> The following systems were studied: (i) Os electrodeposited onto Pt(111), (ii) Os spontaneously deposited onto Au(111), and (iii) an ingot of melted Os powder. In the first procedure, approximately 50 layers of Os were electrodeposited on a Pt(111) substrate from 1 mM OsCl<sub>3</sub> + 0.1 M H<sub>2</sub>SO<sub>4</sub> at 40 mV, and the methanol electrooxidation current was measured at 0.50 V as shown in Figure 11. The current density is still 3 times lower at 23  $\mu\text{A cm}^{-2}$  (of the geometric surface) than that observed for the most active Pt(111)/Os surfaces (75  $\mu\text{A cm}^{-2}$ ). The activity versus the electroactive surface area is quite negligible (2  $\mu\text{A cm}^{-2}$ ), shown as the dashed–dotted line in Figure 11. The electroactive surface area was estimated from the hydrogen adsorption charge to be  $\approx 3 \text{ cm}^2$  (Figure 3). As discussed elsewhere,<sup>40</sup> a Au(111)/Os substrate with  $0.60 \pm 0.06 \text{ ML}$  Os coverage also showed negligible methanol activity. This surface did not show activity either with the as-prepared Os oxides or after reduction of the Os oxides to Os metal. Last, the Os ingot showed little activity at 0.40, 0.50, and 0.55 V (Figure 12). Certainly, the methanol oxidation activity of osmium is small without the proximity to the platinum substrate. These results further support the conclusion that unexposed Pt sites play a necessary role in methanol electrooxidation on Pt(111)/Os.

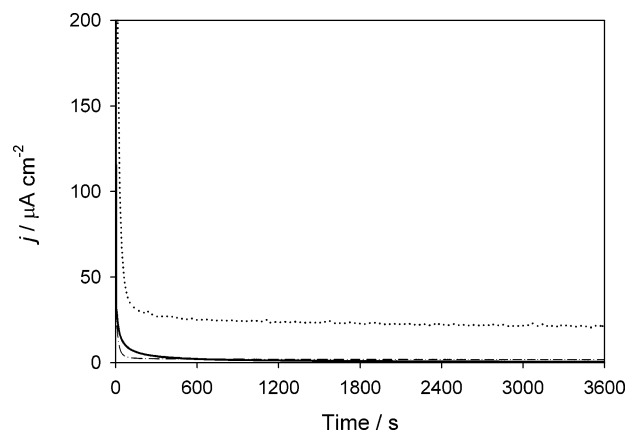


**Figure 11.** Methanol electrooxidation current density–time transients at 0.50 V in 0.6 M CH<sub>3</sub>OH + 0.1 M H<sub>2</sub>SO<sub>4</sub> solution of Os electrodeposits on Pt(111) (CV shown in Figure 3). The solid line corresponds to methanol electrooxidation on the Os-free Pt(111) surface. The dotted line corresponds to methanol electrooxidation on the Os electrodeposits on Pt(111) versus the geometric area of 0.25 cm<sup>2</sup>. The dash–dotted line (nearly superimposed on the Pt(111) data) corresponds to same data as the dotted line, but divided by the estimated electroactive area of 3 cm<sup>2</sup>.

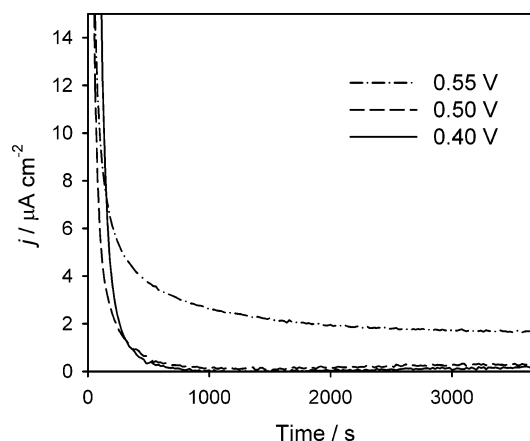


**Figure 12.** Methanol electrooxidation current density–vs.–time transients in 0.6 M CH<sub>3</sub>OH + 0.1 M H<sub>2</sub>SO<sub>4</sub> solution at 0.40, 0.50, and 0.55 V vs RHE obtained for an ingot of melted Os powder. The current at 0.55 V is shown as a dash–dotted line; for 0.50 V, a dashed line; and for 0.40 V, a solid line. The current density is expressed versus the geometric area of Os = 0.5 cm<sup>2</sup>. The real electroactive area is  $\approx 7 \text{ cm}^2$  based on hydrogen adsorption charge.

#### 4. Summary and Conclusions

In this work, the activities of Pt(111)/Os surfaces to CO and methanol were studied as a function of the Os coverage and the type of the substrate. The structural details of the Os deposit were revealed by STM, which showed that Pt sites were still exposed even when the Os packing density = 1. CO oxidation voltammetry on Pt(111)/Os showed a two peak pattern that is quite similar to Pt(111)/Ru, with similar onset potentials for CO electrooxidation. The optimal coverage of Os on Pt(111) for methanol electrooxidation was relatively high at  $0.7 \pm 0.1 \text{ ML}$  ( $1.0 \pm 0.1 \text{ Os packing density}$ ) over a range of potentials from 0.4 to 0.55 V, but the current density decays when the Os coverage is increased beyond this value. This indicates that some Pt sites must be exposed to the methanol solution for the most effective methanol electrooxidation but that the rate-limiting process most likely involves osmium atoms. Either the formation of osmium oxides or the reaction of the osmium oxides with CO may be the rate-limiting process. Methanol electrooxidation studies with homogeneous Pt–Os alloys would further address this question,

(37) Hoster, H.; Iwasita, T.; Baumgartner, H.; Vielstich, W. *J. Electrochem. Soc.* **2001**, *148* (5), A496–A501.

(38) Huang, J.; Yang, H.; Huang, Q.; Tang, Y.; Lu, T.; Akins, D. L. *J. Electrochem. Soc.* **2004**, *151* (11), A1810–A1815.

(39) Zhu, Y. M.; Cabrera, C. R. *Electrochem. Solid-State Lett.* **2001**, *4* (4), A45–A48.

(40) Johnston, C. M.; Strbac, S.; Wieckowski, A. *Langmuir* **2005**, *21* (21), 9610–9617.



since the role (if any) of the osmium atoms in the interior of the osmium islands is unclear.

The evidence for the important role of exposed Pt is strengthened further by the control experiments using osmium electrodeposits (ca. 50 packing density) on Pt(111), Au(111)/Os, and an Os ingot, which all showed poor methanol electrooxidation performances. Overall, the CO oxidation and methanol oxidation results are best explained by the bifunctional mechanism similar to that of Pt(111)/Ru, only with a different optimal balance of Pt and Os sites compared to Pt and Ru sites. Compared to Ru, Os performs poorer at fuel-cell potentials ( $\leq 0.4$  V), and therefore it must have an indirect promoting effect in

the highly active ternary and quaternary alloy catalysts.<sup>6–8,41</sup> However, at higher potentials, the Pt/Os combinations are more active than Pt/Ru.

**Acknowledgment.** This work is supported by the National Science Foundation under Grant NSF CHE03-49999. CJ acknowledges support from a NSF Graduate Research Fellowship.

LA060164E

(41) Gurau, B.; Viswanathan, R.; Liu, R.; Lafrenz, T. J.; Ley, K. L.; Smotkin, E. S.; Reddington, E.; Sapienza, A.; Chan, B. C.; Mallouk, T. E.; Sarangapani, S. *J. Phys. Chem. B* **1998**, *102* (49), 9997–10003.

(42) Johnston, C. M. Ph.D. Dissertation; University of Illinois at Urbana-Champaign: Urbana, IL, 2005.